Contrib Mineral Petrol (1988) 98:444–454

Contributions to Mineralogy and Petrology

Zoned ternary feldspars in the Klokken intrusion: exsolution microtextures and mechanisms*

William L. Brown[1] **and Ian Parsons**[2]

[1] Centre de Recherches Pétrographiques et Géochimiques, BP 20, F-54501 Vandoeuvre-lès-Nancy Cedex, France
[2] Department of Geology and Mineralogy, Marischal College, University of Aberdeen, Aberdeen AB9 1AS, Scotland

Abstract. The microtextures developed during relatively slow cooling as a function of bulk composition in zoned ternary feldspars from syenodiorites and syenites in the Klokken intrusion, described in the preceding paper, were determined by TEM and their origin and evolution deduced. The feldspars normally have a plagioclase core and an alkali feldspar rim; cores become smaller and rims larger and the An content of both decrease with distance from the contact of the intrusion. The following microtextural sequence was observed. The inner plagioclase cores are homogeneous oligoclase-andesine with Albite growth twins only, but are *crypto-antiperthitic* towards the outer core. At first small platelets of low sanidine a few nanometres thick and up to ~10 nm long occur sporadically only on Albite-twin composition planes. With further increase in bulk Or they are homogeneously distributed in the plagioclase. Thicker, through-going plates in platelet-free areas are found, which induce Albite twins in the surrounding plagioclase. The microtextures in the rims are regular cryptomesoperthitic, with ($\bar{6}01$) lenses or lamellae, depending on the bulk Or-content, of low sanidine in Albite-twinned low oligoclase-andesine. Albite and Pericline twins in plagioclase in an M-twin relationship, together with lenticular low sanidine, were found in only one small area. The overall diffraction symmetry of the mesoperthites is monoclinic, showing that exsolution started in a monoclinic feldspar, whereas that of the antiperthites is triclinic. The intermediate zone between the core and rim is more complex and microtextures vary over distances of a few micrometres.

The cryptomesoperthites are very regular where Or-rich and probably arose by spinodal decomposition. The platelets in the outer cores arose by heterogeneous nucleation on twin composition planes and by homogeneous nucleation elsewhere. Near the intermediate zone they coarsened to give larger plates which induced Albite-twins in the plagioclase. Because of the zoning, microtextures that were initiated in areas of given composition, can propagate laterally into zones of different composition. A diagram is given showing the relationship between ternary bulk composition and the microtexture developed in coherent perthitic alkali feldspars and plagioclases from slowly-cooled rocks.

Introduction

Although exsolution microtextures and mechanisms in cryptoperthitic alkali feldspars are well understood (Brown and Parsons 1984a, b; Parsons and Brown 1984; Yund 1984), little is known about exsolution in Ab-rich ternary alkali feldspars and Or-bearing acid plagioclases (Ried and Korekawa 1978). Such feldspars are of special interest because their symmetry, at the start of exsolution, may be monoclinic or triclinic, depending on composition, and this seemed likely to affect the mechanisms of exsolution and the subsequent morphological evolution during coarsening. To eliminate the complication of correlation between crystals of different thermal history, we have studied such meso- and antiperthites in zoned crystals, thus allowing a determination of the effect of composition at fixed cooling rate. A new complication, however, is that the microtextures which develop in one zone may be influenced or even determined by those in adjacent zones. Feldspar crystals with plagioclase cores and alkali feldspar rims are common in syenodiorites and augite syenites of larvikitic affinities from shallow mildly alkaline intrusions. Such crystals may show either apparently smooth simple zoning or abrupt changes and patchy textures in thin section. A detailed study of such zoning patterns is desirable not only for our understanding of the feldspars themselves, but also for that of the evolution of intermediate magmatic rocks.

The transition zone at the outer margin of the unlaminated syenite of the Klokken gabbro-syenite complex, South Greenland (Parsons 1979, 1981; Parsons and Becker 1987) was chosen for a detailed petrographical and mineral-chemistry study covered in a companion paper (Parsons and Brown 1988). The present paper describes the microtextures of some of the zoned feldspars. The main syenite body is intrusive into an outer sheath of gabbro. The outermost two metres of syenitic rocks at the gabbro contact consist of a mafic syenodiorite which grades inwards into a rather structureless leucocratic syenite with rare plagioclase cores to alkali feldspar. Olivine, where present, clinopyroxene and biotite vary systematically, sometimes with compositional gaps, towards the compositions of the same minerals in the inner layered series (Parsons and Becker 1987; Parsons and Brown 1988). From the margin of the syenite intrusion inwards, the feldspars show systematic chemical variation in parallel with that shown by the mafic minerals.

In most of the rocks studied feldspar crystals were composite and two (or three) zones could be distinguished in thin section, an Albite-twinned *plagioclase core*, an outer optically featureless or finely microperthitic *alkali feldspar rim* and in some cases an optically variable *intermediate zone*. The intermediate zone is very much narrower and more irregular than the two other zones. In the marginal syenodiorites the feldspars have well developed calcic ande-

* CRPG contribution 730

Offprint requests to: I. Parsons

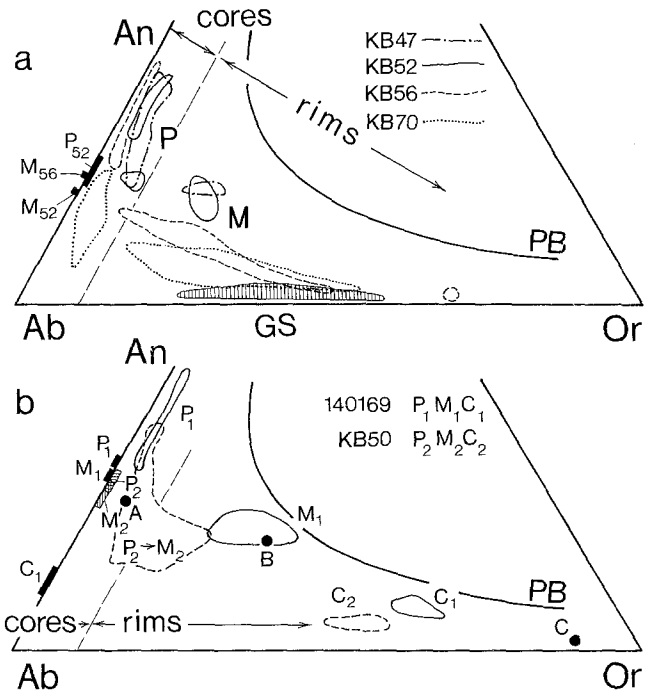

Fig. 1. Bulk compositional variation in feldspars from the Klokken unlaminated syenites. The boxes along Ab-An sideline show compositions of plagioclase phases deduced from γ^*. A straight line at 10% Or separates all areas of plagioclase cores from alkali feldspar rims. Numbers refer to different specimens. **a** Fields showing range of microprobe compositions for feldspars in rocks which are most probably hypersolvus. *P:* plagioclase cores, *M:* alkali feldspar rims (cryptomesoperthites), *GS:* granular syenites (Brown et al. 1983); **b** Fields showing range of microprobe compositions for feldspars from subsolvus rocks. *P:* plagioclase cores, *M:* mesoperthite overgrowths, *C:* cryptoperthite. Solid circles *A, B* and *C* are compositions of areas studied by Ried and Korekawa (1978) – see text

sine-calcic oligoclase cores with thin patchy An-rich alkali feldspar rims of variable Ab/(Ab+Or) ratio which become thicker away from the margin of the intrusion. In the syenites on the other hand, plagioclase cores commonly occur close to the syenodiorite, but become only sporadically present with increasing distance from the contact; they range from andesine to sodic oligoclase but with lower Or contents. Zoning patterns (Fig. 1a; see Parsons and Brown 1988, Fig. 6, for detail) tend to lie near isotherms at the Ab apex of the ternary feldspar system and there is a systematic tendency for compositions to lie near lower-T isotherms on going from the syenodiorites to the unlaminated syenites. Compositions of alkali feldspars in the inner layered syenite series are low in An and close to the Ab–Or minimum; their estimated temperature of crystallization is 900–850° C (Parsons 1981).

In one syenodiorite (KB50) three feldspar compositional ranges were observed (Fig. 1b), an Albite-twinned Or-bearing andesine (P_2), a more-or-less optically featureless Or-poor ternary feldspar (M_2) and an optically featureless Or-rich feldspar (C_2). The three compositions and the optical textures are similar to those observed in a syenogabbro (140169) from close to the outer margin of the gabbro sheath (Fig. 1b), which were shown by TEM (Parsons and Brown 1983; Brown and Parsons 1983) to consist of plagioclase (P_1), a cryptomesoperthite (M_1) and a cryptoperthite (C_1). The two, now perthitic feldspars, from the syenogabbro crystallized together as homogeneous phases in the late stages of crystallization and lie on a high-T isotherm estimated at ~950° C (Parsons and Brown 1983). In a similar way the two feldspars M_2 and C_2 in the syenodiorite crystallized together in the late stages at a T estimated at ~910° C (Parsons and Brown 1988). These rocks were hypersolvus during most of their crystallization history, but became subsolvus in the late stages. Such a third (i.e. Or-rich) feldspar, perhaps present in very small quantities in some of the other syenodiorites, may have been overlooked. All other rocks were entirely hypersolvus.

The rock samples studied came from drill cores in the inner layered syenite series (see Parsons and Brown 1988 for locations) which were cut in two, sections for microprobe analysis and TEM study being made on opposite faces of the cut, so that it was not always possible to study the same crystal. It should be stressed that the compositional ranges obtained by microprobe may not correspond exactly to those of the areas studied by TEM. After optical examination selected areas of suitably orientated zoned feldspars were ion thinned and examined at 200 kV in a JEOL 200CX electron microscope. Electron microprobe analyses (EDS) were made on the other section, only a few semiquantitative analyses being made on the ion-thinned samples in the electron microscope for comparison. Three of the specimens were studied in detail, two syenodiorites (KB50 and KB52) occurring 1.6 and 2.3 m from the outer contact against gabbro, and a syenite (KB56) 11 m from the contact. The compositional range of the zoned feldspars in the three samples spans the high-temperature limit separating feldspars which are triclinic on growth (plagioclase) from those which are monoclinic; they should develop quite different exsolution microtextures. Only plagioclase, mesoperthite and the narrow intermediate zone were studied by TEM, as no separate Or-rich cryptoperthite was found in the ion-thinned foils.

General relationship between composition and symmetry in ternary feldspars

At high temperatures, disordered feldspars are either monoclinic or triclinic and there is a line at each temperature which separates the two fields on a ternary diagram. If cooling is rapid, so that Si,Al ordering does not occur, these lines define a plane near the Ab apex which slopes down towards the Or apex. When projected (Fig. 2) this plane divides the feldspar compositional range into three fields, here called M, T and M→T. Field M corresponds with sanidines, which are monoclinic at all temperatures and field T with plagioclases, which are triclinic at all temperatures. The intermediate field M→T corresponds with feldspars which are monoclinic above the plane and triclinic below and which are called anorthoclase s.l. During the phase transformation they develop Albite or Pericline twinning or more rarely a special combination type known as M twinning (Smith and MacKenzie 1958; McLaren 1978; Gray and Anderson 1982).

If the high-temperature disordered feldspars are cooled down more slowly, both Si,Al ordering and exsolution may occur. In An-free alkali feldspars, exsolution is much more rapid than ordering, as it involves only Na,K interdiffusion. In ternary feldspars both exsolution and ordering involve Si,Al interdiffusion and should occur at more similar rates. The effect of ordering is to raise significantly the temperature of the ternary solvus without greatly affecting, at high T, the position of the surface of the symmetry transformation (Kroll et al. 1980; Kroll and Bambauer 1981). As ordering proceeds, exsolution will start at higher and higher temperatures (for a given bulk composition) and thus the

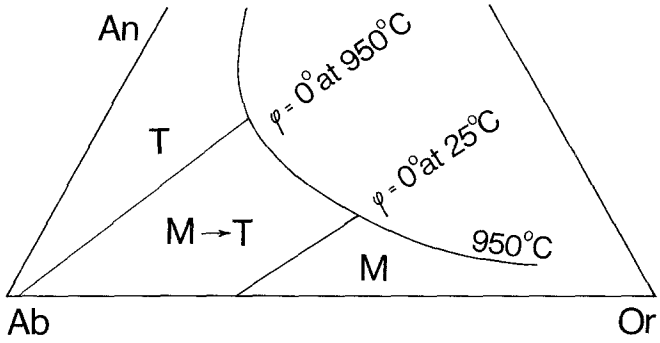

Fig. 2. Fields for disordered feldspars showing symmetry as a function of temperature (rapid cooling). *T:* plagioclase, triclinic at all temperatures; *M:* alkali feldspars, monoclinic at all temperatures; *M→T:* ternary alkali feldspars, which are monoclinic at high and triclinic at low temperatures. The two lines show the symmetry transformation at 25 and 950° C (the temperature of the highest Klokken syenogabbro solidus temperature) and define a plane on which $\varphi = 0°$ which slopes down towards Or

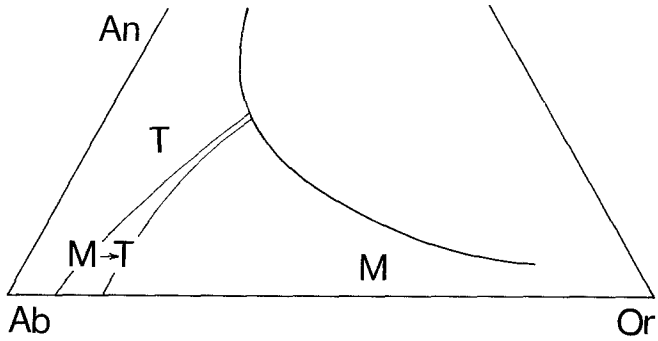

Fig. 3. Fields showing the symmetry of slowly cooled feldspars at the moment of exsolution in the Klokken intrusion. The plane showing the symmetry transformation has intersected the ternary solvus so that the field *M* for feldspars that have monoclinic symmetry when exsolution occurs, extends farther towards Ab. The *M→T* field has therefore shrunk. Field *T* has changed only slightly because of the slight drop in solidus temperatures towards the Ab apex. In field *T* antiperthites develop from triclinic plagioclase and in field *M* mesoperthites and perthites form from monoclinic sanidine. In field *M→T*, unzoned ternary feldspars will undergo the phase transformation and develop twinning before exsolving

field in which exsolution occurs in feldspars with monoclinic symmetry will expand and that with triclinic symmetry will contract. Following very slow cooling ordering may be sufficiently far advanced for feldspars to have an equilibrium or near-equilibrium degree of order. The M→T field of feldspars which develop transformation twins before exsolution shrinks (Fig. 3), and the M field of feldspars which are monoclinic at exsolution, may even come into direct contact with the T or plagioclase field. Furthermore, the exsolution microtextures which develop in feldspars with compositions which lie in each of the three fields will be different, as will the exsolution mechanisms. Depending on the maximum Ab content, zoned crystals may have core compositions which lie in the plagioclase field and intermediate zones which may, or may not, cross the M→T field. In zoned crystals whose compositions cross the field boundaries, twinning and exsolution may be affected by the other zones (see below).

Exsolution microtextures observed as a function of composition

A great variety of microtextures was observed by TEM in the zoned crystals; these were most homogeneously distributed and regular in the alkali feldspar zones and less so where present in the plagioclase cores. They varied very rapidly over short distances (in some cases a few micrometres) in the intermediate zones. This may be related to the irregular patchy compositional variations in some crystals. The microtextures in the alkali feldspar rims, which most resemble previously described cryptomesoperthites, will be dealt with before the more irregular ones.

Alkali feldspar rims – cryptomesoperthite zone

The microtextures in the most Or-rich zones of all the specimens studied are very similar to those already described in An-bearing cryptomesoperthites from larvikites and from the two-perthite alkali gabbro (140169) from the Klokken gabbro sheath (Willaime and Gandais 1972; Brown and Willaime 1974; Willaime et al. 1976; Parsons and Brown 1983). They consist of a largely parallel-sided lamellar intergrowth (Fig. 4a) of Albite-twinned low plagioclase (see below) in the calcic oligoclase range and low sanidine, which shows no sign of incipient transformation to tweed orthoclase. The proportions of the two phases in the Or-rich rims vary in the range 3:1 to 1:1. They are thus true cryptomesoperthites (Smith and Brown 1988). The overall diffraction symmetry is monoclinic and strong streaks join the single low sanidine spot to the Albite twin spots for low plagioclase (Fig. 4b). In areas of lamellar microtexture, the lamellar periodicity is generally in the range 200–400 nm. The interface between the two phases on average is parallel to $\sim(\bar{6}01)$ but shows very regular fine corrugations, which are directly related to the Albite-twin composition planes in the low plagioclase. In detail (Fig. 4c) the interface deviates in a zig-zag way about [106] at each twin plane by up to 20–25° from the trace of the b^* direction, but the outer corners are rounded in order to minimize strain energy (Salje et al. 1985). The sanidine adjacent to the corrugations shows contrast due to elastic strain. In places the interface is slightly offset (Fig. 4a) and suffers enhanced radiation damage due to the probable presence of misfit dislocations (Brown and Parsons 1984b).

Where the bulk Or content is lower, the proportion of plagioclase is greater so that the low sanidine lamellae (Fig. 4a) become discontinuous and wedge-shaped (Fig. 4d) and finally even lens-shaped (Fig. 5a). The Albite twin width or periodicity depends on the local thickness of the individual plagioclase lamella (Fig. 4a), to minimize twin interface and elastic energy, as explained by Willaime and Gandais (1972). Where this thickness varies abruptly, as at the end of a low sanidine lens, the Albite twin periodicity also changes abruptly (Figs. 4d and 5a). In all cases the Albite-twin composition plane extends completely across from one lamella or lens of sanidine to the other. The average interface is generally parallel to b^* in lamellar intergrowths, but where sanidine occurs in lens-shaped areas or where narrow plagioclase bridges occur, the interface may deviate locally therefrom (Figs. 4d, 5b). Oblique lamellae may occur in the intermediate zones (see below).

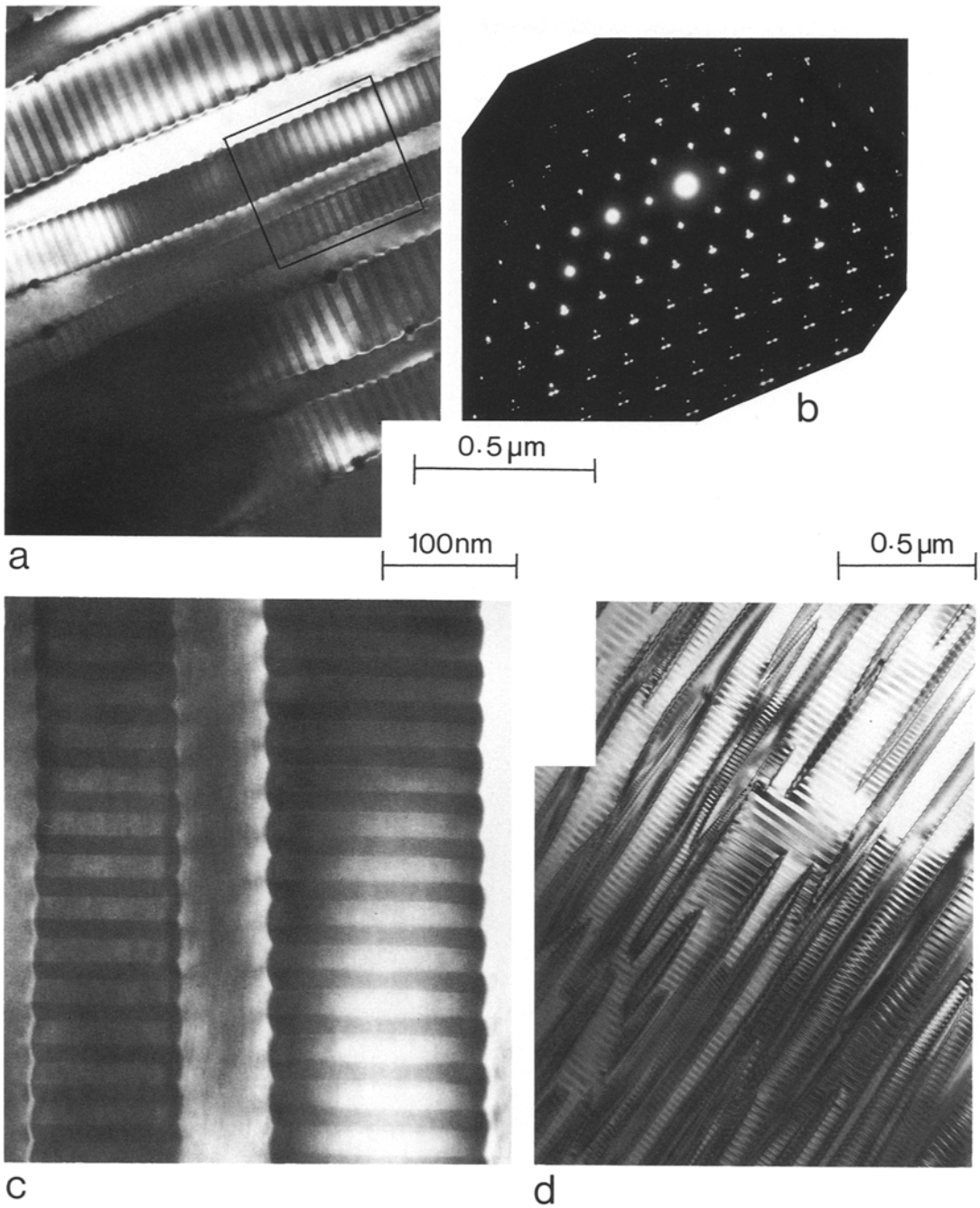

Fig. 4a–d. Bright-field electron micrographs of cryptomesoperthites from the ternary alkali feldspar rims from KB50. Beam parallel to [001]. **a** Lamellar intergrowth of low oligoclase with periodic Albite twins and featureless low sanidine. Interface parallel to $(\bar{6}01)$ with fine corrugations and occasional slight offsets. Small holes due to beam damage may correspond to misfit dislocations; **b** Corresponding diffraction pattern showing single sanidine spots joined by streaks to pairs of Albite-twin spots for low oligoclase; **c** Detail of **a** showing rounded corrugations at Albite twins and associated elastic strain in sanidine; **d** More Or-poor area where low sanidine occurs in lenses parallel to $(\bar{6}01)$. The Albite-twin periodicity varies at ends of lenses

Pericline twins were observed in only one small area of one specimen (KB50). Because of the orientation of the rhombic section in low An_{30} ($\sigma \sim +5°$, Smith and Brown 1988), the Pericline composition plane is not visible in *c*-axis projections. Furthermore, the Pericline twins occurred in proximity to Albite twins in low plagioclase lamellae in an area of lenticular intergrowth parallel to $(\bar{6}01)$ (Fig. 7d). Though the composition planes did not intersect, the diffraction pattern showed that the two twins were geometrically related as in *M twinning* (Smith and MacKenzie 1958). The measured orientation of the Pericline composition plane (Fig. 7d) is $+5$ to $+10°$ showing that the twins developed in an ordered to partly ordered crystal. The volume percentage of plagioclase in these areas is probably $>80\%$ and it occurs with featureless low sanidine.

Plagioclase cores – crypto-antiperthite zone

The microtextures of natural crypto-antiperthites have never been described before. The outer zones of the plagio-

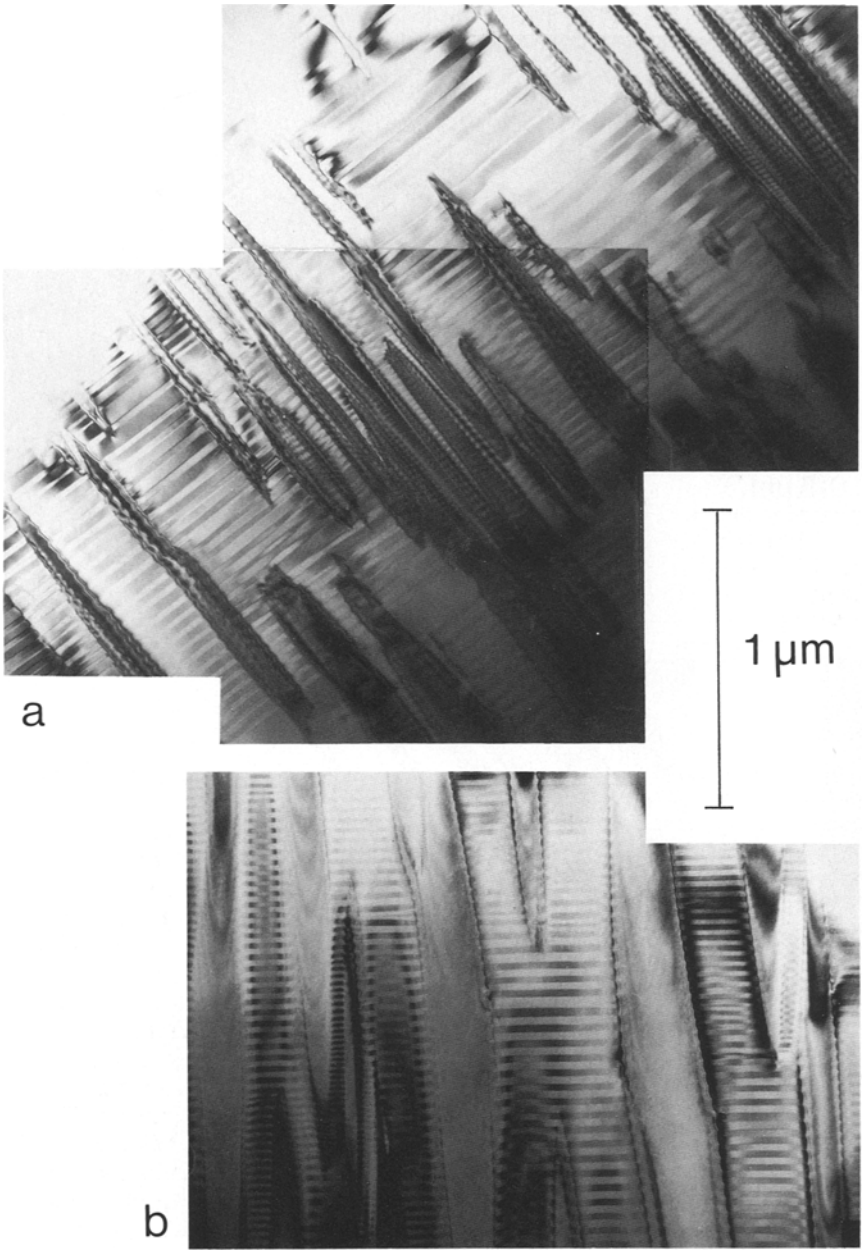

Fig. 5a, b. Bright-field electron micrographs of cryptomesoperthites from KB50. Beam parallel to [001]. **a** Or-poor area with numerous low sanidine lenses in low oligoclase with Albite twins of variable periodicity; **B** More Or-rich area with nearly lamellar texture. Average interface parallel to ($\bar{6}$01) but local deviations around [106] up to 10°, especially where bridges occur

clase cores of all the samples studied are crypto-antiperthitic, whereas the zones near the centre are homogeneous. The only microstructures in the inner cores are Albite growth twins, which are generally wide, always parallel-sided and continuous; the twin widths may vary locally but are only very rarely <1 µm. Farther from the core the average twin width decreases and small 10–100 nm long platelets of an Or-rich feldspar may be observed. These occur at first mainly only on the Albite-twin composition planes (Fig. 6a), and then, in addition, occur distributed homogeneously within one or both of the twin lamellae (Fig. 6b). The Or-rich phase shows up in diffraction patterns as weak streaks associated mainly with one (Fig. 6c) or both of the plagioclase spots, but, because of their very small thickness, the streaks are clearly seen only where the platelets are present in large numbers. The overall diffraction symmetry of the crypto-antiperthites is triclinic. The smallest platelets are 1–2 nm thick when measured on dark-field micrographs. On bright-field micrographs (Fig. 6a), they appear much thicker because of contrast due to coherency strain. They are orientated close to (100); when viewed down c they are inclined to b^*, by an angle of 5–10° (Fig. 6a). As the volume fraction of the Or-rich phase increases, the platelets may give way to larger zig-zag or wing-shaped areas, which have a cusp-like shape at the Albite-twin composition plane (Fig. 6d). Where the platelets are very thin, it is not possible to determine the stress-free symmetry of the Or-rich phase which, because of complete coherency, is elastically constrained to have the same value of γ^* as the plagioclase; the streaks on the diffraction patterns are arranged in the same angular way as the twin spots of the plagioclase (Fig. 6c). Close to the intermediate zone (described next) the density of platelets increases and the thickness of the Albite twins decreases.

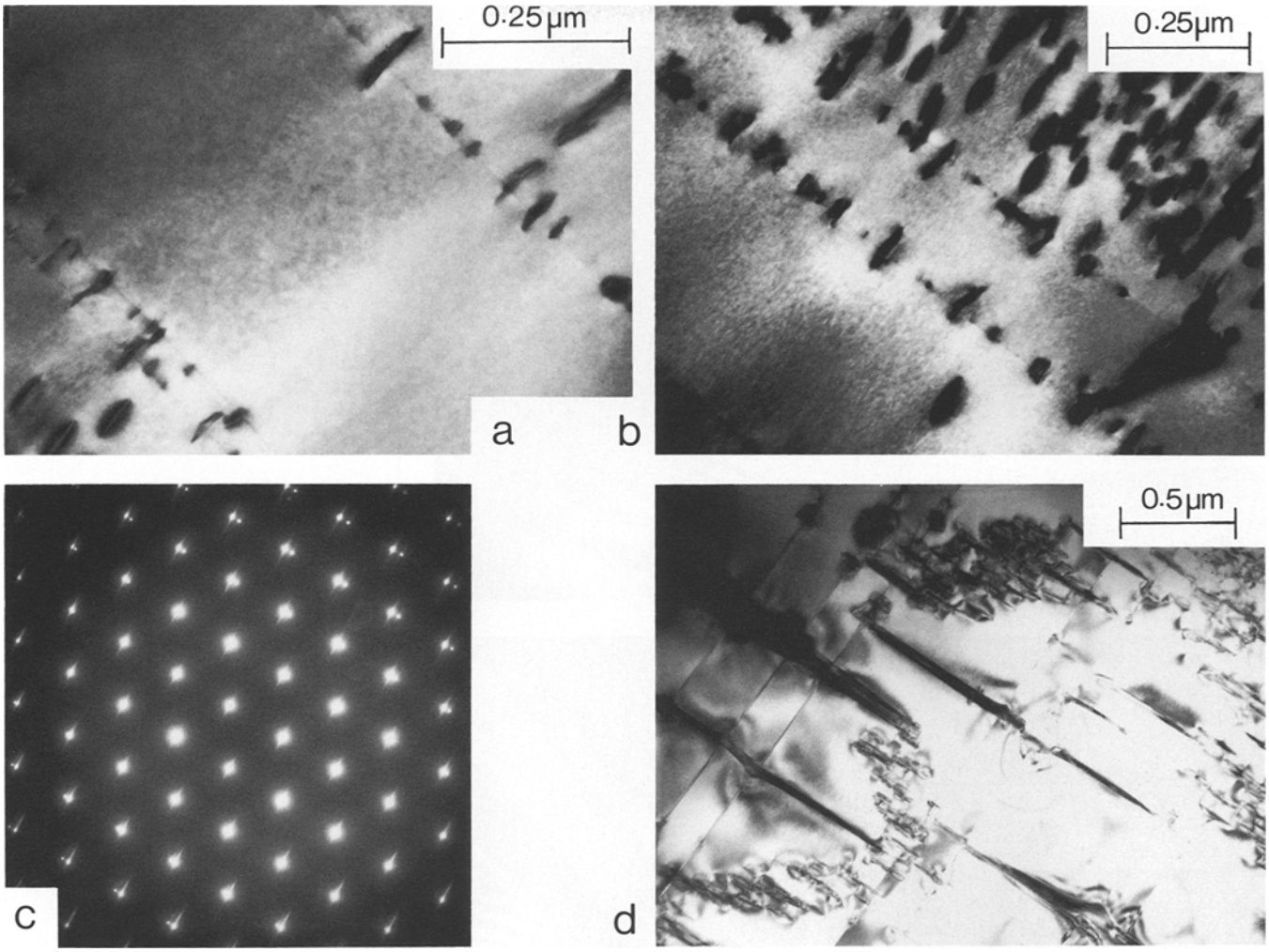

Fig. 6a–d. Bright-field electron micrographs of crypto-antiperthites from outer edges of plagioclase cores. Beam parallel to [001]. **a** Small heterogeneously nucleated platelets of sanidine on Albite-twin composition planes of low oligoclase (faint NW-SE lines, Albite twins not in contrast). Note small homogeneously nucleated sanidine platelets (grey lines, *bottom left*) surrounded by strong elastic strain in plagioclase, resembling coffee beans. KB50; **b** Adjacent area with more abundant homogeneously nucleated platelets in one Albite-twin individual; **c** Diffraction pattern of unbalanced Albite-twinned low oligoclase and strong streaks produced by small low sanidine platelets constrained to be triclinic with same value of γ^* as plagioclase. KB56; **d** Adjacent area with larger plates surrounded by platelet-free areas. Note cusps on plate as it crosses the Albite-twin composition planes (*lower left*)

Intermediate zone

The intermediate zone is characterized by a more-or-less rapid variation in microtexture from that of a plagioclase antiperthite with numerous Or-rich platelets, to that of a regular cryptomesoperthite. There are no sharp boundaries, unlike the situation in the syenogabbro described previously (Parsons and Brown 1983; Brown and Parsons 1983). Part of the irregular variation in composition may be due to incomplete reaction between plagioclase and liquid (Parsons and Brown 1988). The intermediate zone shows large variations in the density of platelets over distances as small as a few micrometres (Fig. 7a), especially where the zone is narrow. Firstly, the platelets coalesce to form larger lenses or even through-going microlamellae, the area immediately adjacent being devoid of small platelets (Figs. 6d and 7b), or if present, they are largely restricted to the Albite twin composition planes (Fig. 7b, c). The larger lenses are frequently associated in groups and may be oblique to b^* (Fig. 7b). These Or-rich lenses induce Albite twins in the plagioclase directly adjacent to the lens. If another lens is close, the twins are parallel-sided and cross from one lens to another. Where the lens is isolated, wedge-shaped Albite twins arise at the interface, but extend out only a distance of 5–15 times their width (Fig. 7b, c). The interface shows corrugations (Fig. 7c) which may be less clearly related to the width of the twin than in the mesoperthites. Where the proportion of Or-rich feldspar increases, normal mesoperthite develops with the lamellar interface parallel to $(\bar{6}01)$. In other circumstances, where the Or-rich lenses were oblique to b^*, an unusual lamellar microtexture is found in which the lamellae may also be oblique to b^* by up to 10° (Fig. 7d).

Proportions, periodicities and phases

The microtextures observed can be only broadly correlated with the compositional variation established separately by

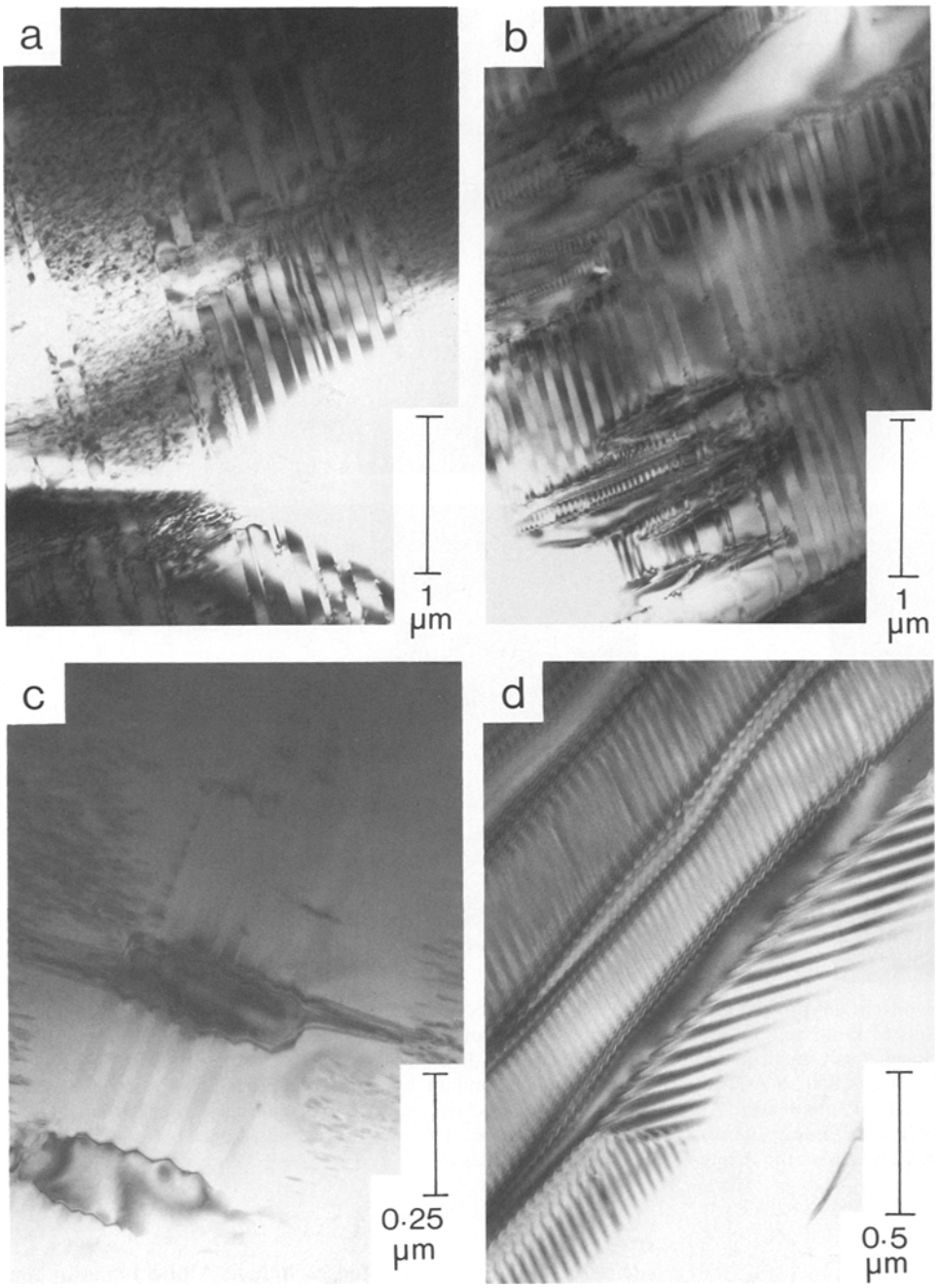

Fig. 7a–d. Bright-field electron micrographs. KB50. **a–c** Intermediate zone. Beam parallel to [001]. **a** Areas rich in homogeneously nucleated platelets adjacent to area with very few; **b** Lenses of low sanidine slightly oblique to *b** together with more irregular areas of sanidine. Note platelets on Albite-twin composition planes; **c** Two small lenses of low sanidine with induced Albite twins in the plagioclase and a corrugated interface. The twins between the two lenses are regular and parallel-sided, whereas they are wedge-shaped outside them with small sanidine platelets at their ends. Many small platelets exist away from lenses; **d** Sanidine lenses parallel to $(\bar{6}01)$ (NE-SW) in Albite-twinned (NNW-SSE) and Pericline-twinned (nearly E-W) plagioclase. Rhombic angle calculated from micrograph +5 to +10°. The twins do not intersect, but occur in M-twin relationship. Electron beam parallel to $[\bar{3}12]$

electron microprobe, as quantitative analysis could not be carried out in the electron microscope. In many cases, textures depend on the *average* composition of volumes of structure which are relatively large compared with the thickness of the lamellae or even with the region imaged by TEM. The proportions of the phases as determined from TEM micrographs give an estimate of bulk composition, which can be correlated with position in the zoned crystals.

All of the cryptomesoperthites had more low plagioclase than low sanidine, a common percentage of plagioclase being in the range 70–55 vol% though some areas had more than 80–85%. In the intermediate zone the volume percentage of sanidine is very variable (Figs. 6d, 7a, b, c) and hard to estimate, but is probably in the range 5–15%. In the crypto-antiperthites the volume percentage of sanidine is probably of the order of a few percent (Fig. 6a, b). The

proportions of phases in the crypto-antiperthites correlate well with microprobe compositions at the An-poor end of the plagioclase (P) trends and those of the intermediate zones with compositions between P and M at the sharp change in trends (Fig. 1; Parsons and Brown 1988, Figs. 6, 7). The proportions of phases in the cryptomesoperthites also correlate well with microprobe compositions. For KB56 in which the microprobe compositions stretch continuously from close to the Ab–An join to beyond Or_{50} near the Ab–Or join (Fig. 1a), the proportion of plagioclase on TEM micrographs varied from ~55–80%. For KB50 the proportion of plagioclase was in the range 62–75% for lamellar microtextures (Fig. 4a, d), but many of the lenticular ones had proportions of ~80% (Fig. 5a) or more corresponding to M_2 on Fig. 1b. It is probable that small areas of the thin foils studied had compositions lying between M_2 and C_2 on Fig. 1b.

Periodicities of exsolution lamellae were very regular in lamellar cryptomesoperthites and were 300 ± 90 nm for KB56 and 260 ± 70 nm for KB50. Non-lamellar "periodicities" were much less regular, the thickness of individual plagioclase bands varying from 0.5–1 μm (Fig. 5a) or more. In some areas of KB52 small regular periodicities of 85 ± 10 nm were observed adjacent to much coarser irregular bands. It is clear that periodicities are only meaningful where regular over large areas. The regular periodicities of 260 nm found in KB50 (1.6 m from margin of the syenite) and 300 nm in KB56 (11 m from margin) are coarser than most of the periodicities observed in the layered series (40–300 nm, Brown et al. 1983) in spite of their much higher An contents. They are intermediate between the values of the mesoperthite and cryptoperthite, of 530 ± 150 and 150 ± 20 nm respectively, in the syenogabbro from near the margin of the gabbro sheath (GGU140169) which have even higher An contents (Parsons and Brown 1983). One possible explanation for the coarseness of the cryptomesoperthites in the syenogabbro, syenodiorites and unlaminated syenites is the much higher temperature of exsolution (850–700° C, see below) compared with those in the An-poor layered syenites (~670° C, Brown and Parsons 1984a); this should be counteracted, however, by the slower coarsening in feldspars with higher An contents.

Phases present were identified from their diffraction patterns and the compositions of the plagioclase phases estimated from γ^* (Fig. 1) on the assumption that they were fully ordered, hence giving maximum values for the An content. Only the maximum values for An are in good agreement with possible compositions from microprobe analyses (Fig. 1). The exsolved plagioclases in the cryptomesoperthites have γ^* near 89.15° (KB56), 89.35° (KB52) and in the range 88.7–89.0° (KB50) corresponding to An_{23}, An_{20} and An_{26-31} respectively; the An content in the mesoperthite from the syenogabbro is in the range An_{30-33} (Parsons and Brown 1983). The plagioclase at the outer limit of the cores has γ^* values of 88.9–89.2° (KB52) and 88.6–88.75° (KB50) corresponding to An_{22-27} and An_{29-33} respectively, the An content in the plagioclase rims of the syenogabbro being An_{33-35} (Parsons and Brown 1983). In each rock the plagioclase in the mesoperthite is slightly less An-rich than that of the outer core or intermediate zone. The An contents for both the exsolved plagioclase in the mesoperthite and in the intermediate zone or outer core decrease from the outer margin of the intrusion inwards in accordance with the decreasing bulk An contents. The exsolved plagioclase from the cryptomesoperthites in the layered series has γ^* near 90° and even lower An contents (Brown et al. 1983). It was not possible to estimate precisely the composition of the exsolved low sanidine in the rims because of the spread of bulk compositions, but by analogy with other perthites (e.g. Parsons and Brown 1983), it probably lies in the range Or_{80-90}; this is in agreement with estimated tie-line relationships (not shown on Fig. 1).

Summary of microtextures

The microtextures can be divided into two groups on the basis of the diffraction symmetry: monoclinic and triclinic. Zones with monoclinic diffraction symmetry (Fig. 4b) have monoclinic low sanidine and balanced Albite-twinned low plagioclase. Zones with triclinic diffraction symmetry have unbalanced Albite-twinned low plagioclase and diffuse streaks radiating inwards from the plagioclase diffraction spots towards the reciprocal lattice origin (Fig. 6c); the Or-rich phase is orientated in reciprocal space in the same way as the plagioclase and is constrained to be triclinic. The centres of the plagioclase cores are homogeneous and consist of low plagioclase with Albite growth twins. The sequence of microtextures from the homogeneous core outwards is:

(a) very small (10–100 nm) rare platelets of Or-rich feldspar occurring on the Albite-twin composition planes (Fig. 6a).

(b) more numerous small platelets distributed homogeneously in one or both of the twin individuals (Figs. 6b, 7a).

(c) larger micrometre-size plates of Or-rich feldspar (Fig. 6d) which extend across several growth twins in a slight zig-zag in areas generally nearly devoid of platelets.

(d) larger through-going lenses of sanidine (Fig. 7b, c) with corrugated interfaces corresponding with wedge-shaped Albite twins in the plagioclase in areas nearly devoid of platelets except on the Albite-twin composition planes. The lenses are sometimes oblique to b^* but are not zig-zag in shape. The centres of the lenses consist of monoclinic low sanidine and the overall diffraction symmetry is nearly monoclinic.

(e) more regular lens-shaped to lamellar microtextures parallel to $(\bar{6}01)$ (Figs. 4, 5a) with monoclinic diffraction symmetry. The plagioclase is almost exclusively twinned on the Albite law with a regular periodicity which depends on the thickness. In one case both Albite and Pericline twins in an M-twin relationship occurred in a plagioclase-rich area with lenses of sanidine parallel to $(\bar{6}01)$ (Fig. 7d).

Microtextures (a) to (c) have triclinic diffraction symmetry and are crypto-antiperthites, (e) has monoclinic diffraction symmetry and is a cryptomesoperthite and (d) is intermediate. In only one area of one specimen were microtextures seen which might possibly have arisen following an unconstrained monoclinic/triclinic transformation (see below, however).

Discussion

The effect of zoning on the development of the microtextures

We now discuss the effect of the zoning on the phase transformation and exsolution mechanisms and development. The crystals grew with a triclinic core and a monoclinic

rim. Sharp boundaries were never seen between the different compositional zones, unlike the situation in the syenogabbro (Brown and Parsons 1983; Parsons and Brown 1983). On cooling the crystals underwent Al,Si ordering and exsolution, and the monoclinic/triclinic transformation front advanced outwards from the core. The cores consist of plagioclase with Albite twins; Pericline twins were not seen in any cores. Consider a zoned crystal with the zoning perpendicular to the (010) plane. At high temperature in a disordered acid plagioclase, the obliquity ($\varphi = b \wedge b^*$) is very small and this decreases to zero as the composition of the crystal varies towards the M→T line (Fig. 2). The Albite twins will extend up to or just beyond the unconstrained M→T transformation front. As the crystal cools, the front will move outwards and at the same time the Albite twins will propagate outwards. M twinning should not develop, as this requires a homogeneous stress field. Even if there is a compositional gap at the M→T front, the phase transformation will still be guided by the long-range strain induced by the Albite twins already present. It is thus probable that zoned crystals, whose composition extends from the T field across the M→T field, will not generally develop M twinning but will inherit twinning by *lateral propagation* from the plagioclase zone. Even when a plagioclase core is absent, M twinning may still not develop in crystals zoned from the M→T field into the M field, if exsolution starts in the latter; exsolution in the M field may induce a long-range strain field beyond the M→T front, which inhibits the formation of M twins. M twins were found only once (Fig. 7d).

Just as for transformation twinning, exsolution in a zoned crystal may be influenced by the strain fields induced by already existing exsolved domains. The zoning patterns in the feldspar are complex. The plagioclase cores show roughly the same variation in An content, from An_{42} to An_{25-20} (or to $\sim An_{10}$ in KB70), with progressively decreasing total Or content from the outer syenodiorites to the unlaminated syenites (Fig. 1); plagioclase cores probably follow simple fractionation paths on the one-feldspar saturation surface at progressively lower *T*. There is then a sharp elbow in the zoning patterns with a nearly linear trend away from the An–Ab sideline across the supposed positions of the solvus isotherms (Fig. 1; Parsons and Brown 1987, Figs. 6, 7). This suggests perhaps that intermediate compositions on the linear trend would exsolve at a higher temperature than the more extreme ones, because zoning paths cross the probable trace of the critical solution curve (ternary solvus crest) (Brown and Parsons 1985), and hence influence the microtextures of some of the other zones. The final crystallization *T* of the subsolvus syenodiorite KB50 is probably ~910° C and for the hypersolvus syenites in the range 910–850° C (Parsons and Brown 1988). Exsolution temperatures from central to extreme compositions were probably of the order of 850–700° C (cf. Parsons and Brown 1983). It is probable that exsolution textures in the intermediate zone were influenced by those in the plagioclase cores and the mesoperthite rims.

Ried and Korekawa (1978) reported a microprobe and TEM study of a "moonstone" of unknown origin from Labrador. Optically it had an irregular texture and consisted mainly of a finely twinned basic oligoclase (bulk composition $An_{27.2}Ab_{69.2}Or_{3.6}$, Fig. 1b, point A), and a smaller amount of a featureless feldspar (B) with, in part, undulose extinction (bulk composition, measured by EDS

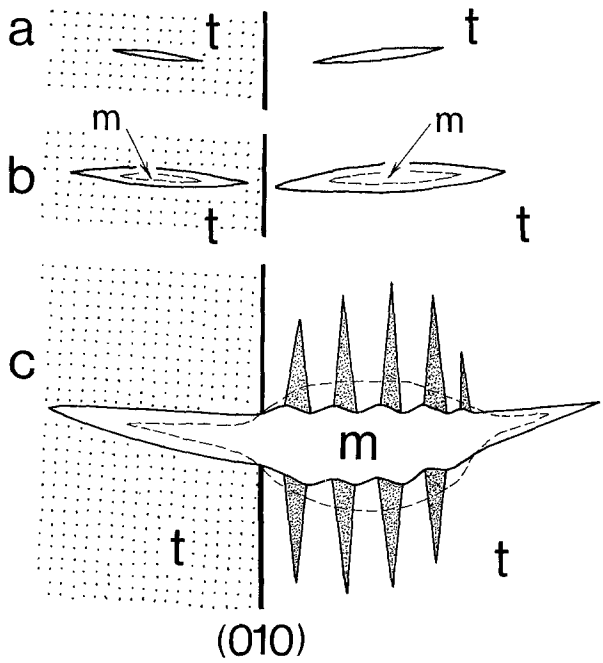

Fig. 8a–c. Schematic diagram showing stages in development of a lens (**c**) of low sanidine with induced Albite twins (heavy stipple) in plagioclase and corrugated interface, developed from a small platelet (**a**). The heavy line, (010), is the composition plane of an Albite growth twin, shown by light stipple. **a** The sanidine platelet is elastically constrained to be triclinic (t) by surrounding plagioclase (cf. *Fig. 6a, c*); **b** The platelet is larger and its centre has relaxed to monoclinic (m) symmetry; **c** The through-going lens has induced wedge-shaped Albite twins in the plagioclase and the average monoclinic/triclinic front has moved into the plagioclase (cf. *Figs. 7c, 4c*)

in the electron microscope, $\sim An_{20}Ab_{50}Or_{30}$, point B) and small amounts of an Or-rich feldspar ($An_2Ab_{10}Or_{88}$, point C). It is not possible to determine either the relationships between the various components of this complex feldspar or their possible origin(s) as no optical micrograph was given; part C may be a deuterically unmixed part of B. Parts A and B were studied by TEM (Ried and Korekawa 1978). Plagioclase (A) is homogeneous and finely twinned on the Albite or Pericline laws, and in places the two intersect giving M twinning. It has a most unusual reported composition to have developed M twins. Part B is a mesoperthite with ~60% plagioclase by volume, the Or-rich lamellae being parallel to $(\bar{8}01)$ with highly variable thickness (15–1500 nm) in different parts. The plagioclase lamellae are twinned on the Albite or Pericline laws. The microtextures of this composite feldspar of unknown origin are more complex and irregular than those from Klokken. There may be parts which underwent the monoclinic-triclinic transformation before or at the same time as exsolution and hence influenced exsolution in other parts of the crystals.

Origin of the microtextures in the different zones

Alkali feldspar rim. Exsolution in the cryptomesoperthites developed by spinodal decomposition and coarsening in the range 850–700° C within an originally monoclinic partly ordered sodian sanidine (Brown and Parsons 1983, 1984a). Periodic Albite twinning developed at lower *T* in the ex-

solved plagioclase to minimize strain energy. Because of the relatively high An content, the average exsolution interface remained parallel to ~($\bar{6}$01) and misfit dislocations developed, rather than large-scale interface rotation (Brown and Parsons 1984b). At still lower T small-scale corrugations developed along the interface at the Albite twins in the plagioclase (Fig. 4c). The local interface adopted a position of minimum strain for each twin, which is probably close to the calculated positions of ($\bar{6}$31) to ($\bar{3}$31) obtained for low sanidine and untwinned acid plagioclase or anorthoclase (Willaime and Brown 1974; Fleet 1982), though the signs of the indices were not checked by high-resolution electron microscopy (Willaime and Brown 1985). The major variation in the textures is in the proportions of the two phases, Or-poor zones having lens-shaped rather than lamellar sanidine. In the Klokken suite, only in one area with lenticular sanidine, in sample KB50, were M twins observed (Fig. 7d). This Or-poor area may either have undergone the M→T transformation before exsolution or both Albite and Pericline twins developed around the exsolved sanidine lenses. This latter alternative is supported by the angle of the Pericline twin plane (+5 to +10°) which shows that the twins developed in an ordered feldspar rather than a disordered one (−5°) (Smith and Brown 1988) and hence that the twins developed after exsolution at a lower T during ordering.

Plagioclase cores. The plagioclase cores have Or contents which increase outwards, but do not exceed ~7%. They increase towards the intermediate zone with fractionation, but the average Or contents decrease from the syenodiorites to the syenites. Exsolution is absent from the central parts of the cores and is increasingly present towards the outer parts. Or-rich feldspar occurs first as platelets restricted to zones along the Albite-twin composition planes (Fig. 6a); these platelets formed by heterogeneous nucleation. Where more abundant, the platelets are homogeneously distributed and arose by homogeneous nucleation (Figs. 6b, 7a). They are similar to, but less close together than, those seen at intracrystalline boundaries in a mesoperthite from the alkali-gabbro sheath (Brown and Parsons 1983). The density of platelets increases and larger plates or thin, slightly zig-zag lamellae appear towards the intermediate zone (Fig. 6d). The plagioclase next to these plates or thin lamellae is unusual in two ways. Firstly, it is always devoid of Albite twins along the interface. This can be explained by the fact that the plates are too thin (a few nanometres) to have adopted monoclinic symmetry, and so they have not induced twins in the plagioclase. Secondly, it is usually devoid of homogeneously nucleated platelets; this can be explained in two ways depending on the relative ages of the plates and platelets. If the plates grew first at higher T, they would drain the surrounding volume of Or and stop homogenous nucleation at lower T. If the platelets grew first, then the plates (which are larger) could form from them by coarsening, hence producing the platelet-free zone. Both alternatives can be reconciled with the presence of heterogeneously nucleated platelets along the twin composition planes. The exact mechanism may depend on the frequency of Albite twins. Where Albite twins are widely spaced, homogeneous nucleation is favoured, whereas heterogeneous nucleation is favoured where the twin widths are very small. We prefer the second alternative because in a cooling intrusion the times for each successive temperature range increase as T decreases. It is not possible at present to estimate these temperatures.

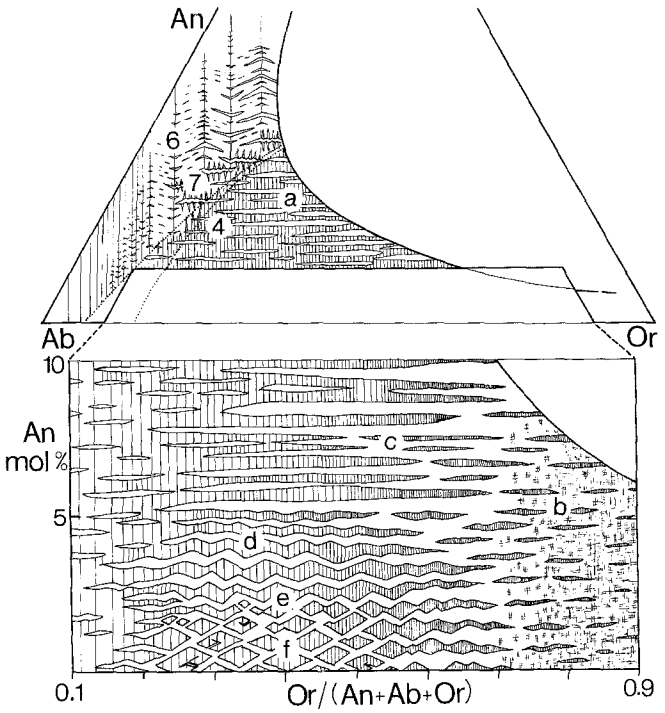

Fig. 9. Schematic diagram showing microtextures, viewed down [001], developed as a function of composition in slowly cooled ternary feldspars. *Vertical lines* are Albite-twin composition planes in plagioclase. Tweed orthoclase is shown by *cross hatching;* it may develop in more Ab-rich straight lamellar intergrowths but is particularly characteristic of the Or-rich compositions shown. Remaining potassium feldspar is shown unornamented, but is low sanidine in straight lamellar intergrowths, high microcline in wavy intergrowths, and low microcline in well-developed zig-zag and lozenge intergrowths. Short period corrugations at the boundaries between albite twins and potassium feldspar lamellae are shown in the vicinity of the M→T symmetry transformation (*dotted lines,* see Fig. 3) but are omitted for simplicity elsewhere. Considerable artistic licence has been applied in the drawing: the obliquity of Albite twins in plagioclase is exaggerated, the scale of microtextures and relative proportions of the phases are very rough and the periodicity of Albite twins in plagioclase in the meso- and cryptoperthites, which depends on local perthite lamellar thickness, is shown in only a generalized way. Albite growth twins in oligoclase also tend to be relatively thin, as shown. Numbers refer to Figures in the present paper. Letters refer to illustrations in earlier papers, as follows: *a Fig. 5* and *b Fig. 6* in Parsons and Brown (1983, *c* and *d Fig. 3* in Brown and Parsons (1984a), *e Fig. 5* and *f Fig. 6* in Brown et al. (1983)

Intermediate zone. This zone is volumetrically restricted and has been strongly influenced by the other two. It is characterized by the presence of larger (up to 5 μm long) sanidine lenses which have monoclinic symmetry and which have induced Albite twins, frequently wedge-shaped, in the adjacent plagioclase. They may be parallel to b^* (Fig. 7c) or be oblique thereto by 10–20° (Fig. 7b). Their origin may be as follows. Like the plates, they probably arose by nucleation and growth. During growth they would extend both at the front and at the side. When thin they are constrained by coherency stresses to be triclinic with an obliquity close to that of the plagioclase (Figs. 6c, 8a). As they thicken,

coherency stresses will relax and the obliquity will decrease from the interface to the centre of the lens until it reaches zero (Fig. 8b). As the central monoclinic part thickens, the misfit along the interface and the total strain increase. The total strain can then be reduced by the formation of periodic wedge-shaped twins in the plagioclase, with small-scale corrugations on the interface, and the rotation of the average interface towards b^* (Fig. 7c). During growth the limiting surface of the volume with monoclinic average symmetry should move from inside the Or-rich feldspar (Fig. 8b) to inside the plagioclase (Fig. 8c). It is more difficult to explain why some of the lenses are oblique to b^* (Fig. 7b). It might be that they arose in an area where only one plagioclase orientation was present originally and that rotation was not completed, but this is not entirely satisfactory.

Finally, Figure 9 is a schematic summary diagram showing the relationship between bulk composition and microtexture. It is based on the present observations and on data from the feldspars from the Klokken layered series and elsewhere (Brown and Parsons 1984b). It requires extension to more An-rich and to more Ab-rich compositions and also to feldspars which have undergone the monoclinic-triclinic transformation before exsolution.

Acknowledgements. The authors thank CNRS (WLB) and NERC (IP) for financial support and the NATO Scientific Affairs Division for generous travel funds.

References

Brown WL, Parsons I (1983) Nucleation on perthite-perthite boundaries and exsolution mechanisms in alkali feldspars. Phys Chem Mineral 10:55–61

Brown WL, Parsons I (1984a) Exsolution and coarsening mechanisms and kinetics in an ordered cryptoperthite series. Contrib Mineral Petrol 86:3–18

Brown WL, Parsons I (1984b) The nature of potassium feldspar, exsolution microtextures and development of dislocations as a function of composition in perthitic alkali feldspars. Contrib Mineral Petrol 86:335–341

Brown WL, Parsons I (1985) Calorimetric and phase diagram approaches to two-feldspar geothermometry: a critique. Am Mineral 70:356–361

Brown WL, Willaime C (1974) An explanation of exsolution orientations and residual strain in cryptoperthites. In: MacKenzie WS, Zussman J (eds). The feldspars, Manchester Univ Press, pp 440–459

Brown WL, Becker SM, Parsons I (1983) Cryptoperthites and cooling rate in a layered syenite pluton: a chemical and TEM study. Contrib Mineral Petrol 82:13–25

Fleet ME (1982) orientation of phase and domain boundaries in crystalline solids. Am Mineral 67:926–936

Gray NH, Anderson JB (1982) Polysynthetic twin width distributions in anorthoclase. Lithos 15:27–37

Kroll H, Bambauer H-U (1981) Diffusive and displacive transformations in plagioclase and ternary feldspar series. Am Mineral 66:763–769

Kroll H, Bambauer H-U, Schirmer U (1980) The high albite-monalbite and analbite-monalbite transitions. Am Mineral 65:1192–1211

McLaren AC (1978) Defects and microstructures in feldspars. Chem Phys Solids Interfaces, Chem Soc London, 7:1–30

Parsons I (1979) The Klokken gabbro-syenite complex, South Greenland: cryptic variation and origin of inversely graded layering. J Petrol 20:653–694

Parsons I (1981) The Klokken gabbro-syenite complex, South Greenland: quantitative interpretation of mineral chemistry. J Petrol 22:233–260

Parsons I, Becker SM (1987) Layering, compaction and post-magmatic processes in the Klokken intrusion. In: Parsons I (ed) Origins of Igneous Layering. Reidel, Dordrecht, pp 29–92

Parsons I, Brown WL (1983) A TEM and microprobe study of a two-perthite alkali gabbro: implications for the ternary feldspar system. Contrib Mineral Petrol 81:1–12

Parsons I, Brown WL (1984) Feldspars and the thermal history of igneous rocks. In: Brown WL (ed) Feldspars and feldspathoids. Reidel, Dordrecht, pp 317–371

Parsons I, Brown WL (1988) Sidewall crystallization in the Klokken intrusion: zoned ternary feldspars and coexisting minerals. Contrib Mineral Petrol 98:431–443

Ried H, Korekawa M (1978) Twinning and exsolution in an antiperthite. Phys Chem Mineral 3:263–270

Salje E, Kuscholke B, Wruck B (1985) Domain wall formation in minerals I: theory of twin boundary shapes in Na-feldspar. Phys Chem Mineral 12:132–140

Smith JV, Brown WL (1988) Feldspar minerals, vol. 1. Springer, Berlin Heidelberg New York Tokyo

Smith JV, MacKenzie WS (1958) The alkali feldspars IV. The cooling history of high-temperature sodium-rich feldspars. Am Mineral 43:872–889

Willaime C, Brown WL (1974) A coherent elastic model for the determination of the orientation of exsolution boundaries: application to the feldspars. Acta Crystallogr A30:316–331

Willaime C, Brown WL (1985) Orientation of phase and domain boundaries in crystalline solids: discussion. Am Mineral 70:124–129

Willaime C, Gandais M (1972) Study of exsolution in alkali feldspars. Calculation of elastic stresses inducing periodic twins. Phys Stat Sol (a) 9:529–539

Willaime C, Brown WL, Gandais M (1976) Physical aspects of exsolution in natural alkali feldspars. In: Wenk H-R (ed) Electron microscopy in mineralogy. Springer, Berlin Heidelberg New York

Yund RA (1984) Alkali feldspar exsolution: kinetics and dependence on alkali interdiffusion. In: Brown WL (ed) Feldspars and feldspathoids. Reidel, Dordrecht, pp 281–315

Received July 28, 1987 / Accepted January 25, 1988

Editorial responsibility: J. Hoefs